Space Sci Rev (2010) 151: 159–181
DOI 10.1007/s11214-009-9602-x

The LISA Pathfinder Mission

Tracing Einstein's Geodesics in Space

Giuseppe D. Racca · Paul W. McNamara

Received: 22 December 2008 / Accepted: 2 November 2009 / Published online: 15 December 2009

Abstract LISA Pathfinder, formerly known as SMART-2, is the second of the European Space Agency's Small Missions for Advance Research and Technology, and is designed to pave the way for the joint ESA/NASA Laser Interferometer Space Antenna (LISA) mission, by testing the core assumption of gravitational wave detection and general relativity: that free particles follow geodesics. The new technologies to be demonstrated in a space environment include: inertial sensors, high precision laser interferometry to free floating mirrors, and micro-Newton proportional thrusters. LISA Pathfinder will be launched on a dedicated launch vehicle in late 2011 into a low Earth orbit. By a transfer trajectory, the sciencecraft will enter its final orbit around the first Sun-Earth Lagrange point. First science results are expected approximately 3 months thereafter.

Here, we give an overview of the mission including the technologies being demonstrated.

Keywords LISA Pathfinder · Gravitational waves · Inertial sensing · Laser metrology · Charge management · Micro-Newton thrusters · FEEPS · Colloids · DFACS

PACS 04.80.Nn · 95.30.Sf · 95.55.Ym

1 LISA Pathfinder—A Technology Precursor of LISA

The LISA Pathfinder mission is a precursor to the joint ESA/NASA Laser Interferometer Space Antenna (LISA) mission. LISA is a constellation of three spacecraft devoted to detect and observe gravitational waves (GW) in the frequency band of 10^{-4} to 10^{-1} Hz. Gravitational waves are ripples in the curvature of spacetime produced by a time variation of the

G.D. Racca (✉)
LISA Pathfinder Project Manager, European Space Agency - ESTEC, Keplerlaan 1,
2201 AZ Noordwijk, The Netherlands
e-mail: giuseppe.racca@esa.int

P.W. McNamara
LISA Pathfinder Project Scientist, European Space Agency - ESTEC, Keplerlaan 1,
2201 AZ Noordwijk, The Netherlands
e-mail: Paul.McNamara@esa.int

gravitational field of massive celestial bodies. GW are characterised by an amplitude, h, which is related, at the *detector side*, to the caused change of proper distance between two spacetime events by the following relation:

$$h = 2\frac{\delta l}{l} \tag{1}$$

where l is the separation between the two spacetime events and δl is the variation of it caused by the passage of the GW. Equation (1) shows the tidal nature of the GW effects which produce length changes proportional to size. At the *source side*, the GW amplitude is related to the variation of the mass properties of the emitting body, by the following approximate equation, called the quadrupole formula, valid for systems where the velocities are non-relativistic:

$$h = \frac{2G}{c^4}\frac{1}{r}\frac{\partial^2 Q}{\partial t^2} \tag{2}$$

where G is the universal gravitational constant, c is the speed of light in vacuum, r is the distance from the source to the detector, and Q is the second moment, or quadrupole moment, of the source mass distribution. The term $\frac{2G}{c^4} \approx 10^{-44}$ in SI units is responsible for the very low numerical value of the GW amplitude. As an example, a compact binary system of two $1\,\mathrm{M}_\odot$ objects at a distance of 1 kpc, gives a strain amplitude of only $h \approx 10^{-22}$. Recalling (1), one can deduce that unless l is huge, the variation δl will be very small. As we will see later in LISA, l is in the order of 5 million km, hence the detector must be capable of measuring δl in the order of few tens of picometres.

Gravitational waves are a direct consequence of Albert Einstein's theory of gravitation (1915) (Einstein 1916), or general relativity, and the existence of gravitational radiation propagating at the speed of light was predicted by Einstein himself. Gravitational waves, as all other forms of radiation, carry energy. Especially massive and compact objects, like compact binaries and black holes at relativistic speeds emit a huge amount of radiation. This has caused the first indirect detection of gravitational wave by Hulse and Taylor in 1975 (Hulse and Taylor 1975). They observed the inspiral of the neutron star binary pulsar PSR 1913+16 and calculated the energy loss due to escaping gravitational waves corresponding to Einstein's theory prediction to 0.3%.

An important feature of the gravitational waves is their frequency band. For compact sources, the GW frequency band is related, through the quadrupole formula (see (2)), to the source size, or lengthscale over which the source dynamics vary, and to the source mass. It can be seen that the frequency band has an upper limits at about 10^4 Hz, corresponding to emissions from very compact sources of several solar masses and Schwarzschild radius lengthscale. On the lower side, the low frequency band $10^{-5} \leq f \leq 1$ Hz, emissions are from compact sources of thousands to millions solar masses or widely separated solar mass bodies. The GW are predicted at even much lower frequency, oscillating on scales comparable to the size of the universe. These GW have been described as "smoking gun" signature of the early universe inflation. Figure 1 shows in a pictorial way strain and frequency characteristics of typical sources.

While the high frequency band is explored by ground based detectors, the low frequency GWs cannot be detected from ground, as it is impossible to completely isolate the instruments in this frequency range from local ground motions. This is the realm of the space-borne detectors. Gravitational wave detection in space is based on the possibility to accurately track two distant proof masses travelling on a *geodesic*. If we place two test particles in space and we shield them from any external force acting on them, they will follow two geodesics. If the spacetime is relatively smooth, such that e.g. the geodesics do not cross,

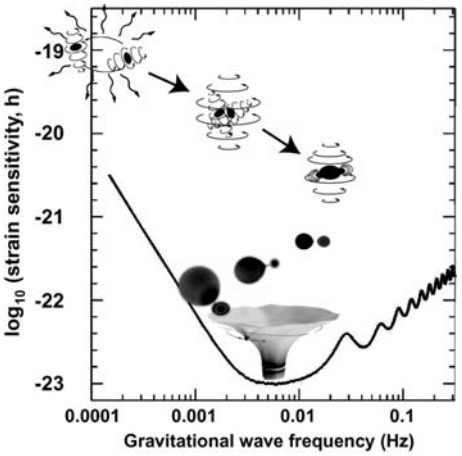

Fig. 1 Expected strain and frequency of gravitational waves emitted by typical sources

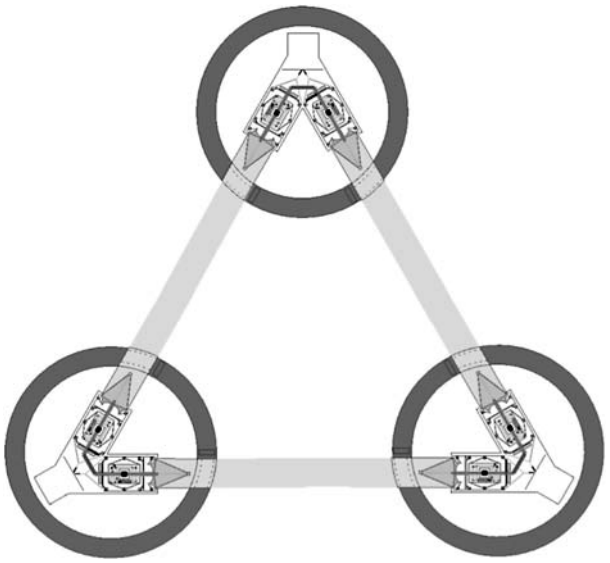

Fig. 2 LISA constellation and laser beams configuration

the two particles will move with no relative acceleration. However, if a GW travels in the neighbourhood of the test particles, a tidal effect will show up, according to (1) and produce a distance change between the particles. In order to detect such a change, a method to track the test masses is necessary. We can do that by means of a laser beam exchanged between the two particles during their motion on the geodesics and measure the distance variation by phase measurement with a heterodyne interferometer.

This concept is realised in practice in LISA. The free falling particles are cubic test masses hosted by a proper housing inside a spacecraft. LISA consists of an equilateral triangular constellation of three spacecraft orbiting at 1 AU from the Sun, lagging behind the Earth by about 20°, corresponding to a distance of 50 million km from the Earth. Each spacecraft hosts two test masses which act as mirrors reflecting a laser beam coming from one of the other spacecraft; see Fig. 2 for clarity. In this way three arms are formed, effectively functioning as a Michelson interferometer with a redundant third arm. The arm length size of about 5 million km was chosen to optimise the sensitivity at the frequency of

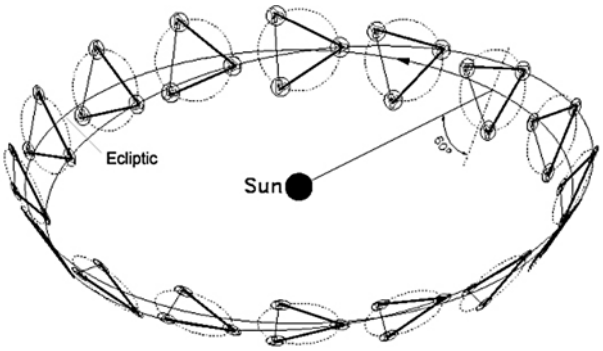

Fig. 3 LISA constellation orbit around the Sun

known GW sources, as increasing the arm length improves the sensitivity to low frequency GW. Each spacecraft is to provide the protection against the external disturbances for the test masses and to accommodate the spacecraft subsystems, including the *Drag-Free Attitude Control System (DFACS)* needed to maintain the test masses in as pure as possible free fall. The spacecraft constellation rotates around its centre of mass on a plane tilted 60° with respect to the ecliptic plane (see Fig. 3). A clever choice of the orbit parameters allow the formation to complete a full rotation around the centre of the triangle, while completing a full revolution around the Sun.

From the above schematic description of the LISA mission, it is clear that two key features are required for the realisation of such a device. The first is related to the concept of *geodesic*, or better to its practical realisation. The capability to shield a test mass from all external forces, while hosting it into a spacecraft which needs to be launched into space, manoeuvred and controlled requires techniques and technologies which have never been experimented before. The second aspect is related to the extremely small distance measurements—in the order of picometres—required to be performed by an on-board interferometer. The demonstration in flight of these two enabling technologies for LISA is the objective of the LISA Pathfinder mission.

2 LISA Pathfinder Science Case

The main aim of the LISA Pathfinder mission is to demonstrate, in a space environment, that free-falling bodies follow geodesics in space–time by more than two orders of magnitude better than any past, present, or planned mission (with the exception of LISA itself) (Vitale et al. 2007).

In Einstein's general theory of relativity, gravity is not considered as an external force: instead gravity is the source of spacetime curvature. Therefore, in a universe devolved of mass (a flat spacetime), free-falling test masses will move in straight lines with uniform velocity (Newton's first law). However, in the real (as described by general relativity) Universe, the presence of mass, hence gravity/curvature, modifies Newton's first law to state that in the absence of any external force, free-falling test masses move along geodesics. The concept that a particle falling under the influence of gravity alone follows a geodesic in space-time is at the very foundation of general relativity; all experiments aimed at demonstrating a prediction of GR require the use of particles that are, to varying accuracies, in geodesic motion.

Examples of such experiments include: MICROSCOPE (Touboul et al. 2001), STEP (Mester et al. 2001), and GG (Nobili et al. 1996) which are designed to test the weak equivalence principle; Viking (Resenberg et al. 1979) and Cassini (Bertotti et al. 2003) which have made measurements of the Shapiro time delay; LATOR (Turyschev et al. 2004) and

ASTROD (Ni 2002), both of which propose to measure to high accuracy post-Newtonian parameters; GP-B (Buchman et al. 2000) a mission to directly measure the effects of frame-dragging, and finally LISA (Shaddock 2008), and the ground-based gravitational wave detectors (LIGO (Abramovici et al. 1992), VIRGO (Acernesse et al. 2004), GEO 600 (Danzmann et al. 1992), and TAMA (Takahashi et al. 2004). In all these experiments, curvature is studied through its effect on some aspect of the motion of particles along geodesics.

The difficulty of achieving high purity geodesic motion is that any parasitic forces compete with spacetime geometry to set masses into motion, perturbing them away from their geodesic lines. As gravity is by far the weakest of all fundamental interactions, achieving the required extremely low level of non-gravitational acceleration requires the understanding, reduction, and control of the disturbances produced by a wide range of physical phenomena. The LISA Pathfinder experiment concept is to improve the uncertainty in the proof of geodesic motion. This is achieved by tracking, using pico-metre resolution laser interferometry, two test-masses nominally in free-fall (Fig. 8), and by showing that their relative parasitic acceleration, at frequencies around 1 mHz, is at least two orders of magnitude smaller than anything demonstrated or planned so far.

To reach its goals, LISA Pathfinder will have to achieve many *firsts* simultaneously. Its test masses will be the first large-mass high-purity metal test bodies flown freely in space at a distance of several millimetres from their immediate surroundings and with no mechanical contact to them. With its test mass to test mass and test mass to spacecraft interferometric motion readout, it will realize the first high precision laser interferometric tracking of orbiting bodies in space. With its nanometer spacecraft to test-mass control and its pico-metre test mass to test mass control, it will realize the first nano and sub-nanometer formation flight of bodies in orbit. And with its sub nano-g self-gravity suppression at both test masses locations, it will be the first high-quality orbiting gravitational laboratory for fundamental physics missions.

The concept of LISA Pathfinder is derived from the classical Einstein *Gedanken* experiment depicted in Fig. 4. In this thought experiment, the curvature of spacetime can be measured by exchanging a photon between two free-falling particles moving along geodesics. The rate of change of the frequency of the photon then gives a direct measure of the spacetime curvature between the particles according to following relationship:

$$\frac{1}{\omega_{\text{light}}}\frac{d\omega_{\text{light}}}{dt} \approx cR^{1}_{010}\Delta x^{1} \tag{3}$$

where ω_{light} is the angular frequency of the photon, Δx^1 is the separation between the particles (along x^1) and $R^{\eta}_{\alpha\beta\gamma}$ is the Riemann–Christoffel tensor, which represents the real effect of matter-energy on spacetime geometry.

This thought experiment is the basis for all gravitational wave detectors; the passage of a gravitational wave appears as a change in the curvature of the spacetime between the particles. In LISA, the free-particles are gold-platinum cubes located in the spacecraft at the ends of the 5 million kilometre arms, while in the ground based detectors, the free-particles are represented by the suspended mirrors at the end of the interferometer arms. However, in LISA Pathfinder, the goal is *not* to measure the curvature of spacetime, instead the goal is to demonstrate the underlying assumption of the *gedanken* experiment: free-particles move along geodesics. As such, the *armlength* between the test masses is significantly reduced compared to, say LISA, (in this case to 38 cm), thereby removing the effects of spacetime curvature on the frequency of the light.

Unfortunately, in a real experiment, not only spacetime curvature or the tidal effect of the passage of a gravitational wave affect the frequency of the light; the frequency also

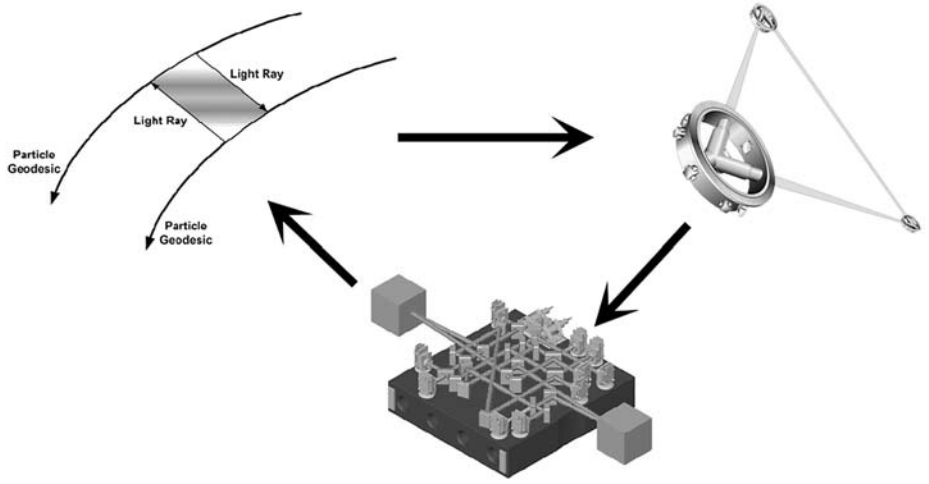

Fig. 4 LISA Pathfinder experiment concept. The top left image shows the classical Einstein thought experiment to measure spacetime curvature. This is the basis for all gravitational wave detectors, e.g. LISA (*top right*). LISA Pathfinder will not only pave the way for LISA, but will also demonstrate the main assumption of the thought experiment: that free particles follow geodesics

changes due to many other effects, most notably due to secular variations of the orbital motion inducing Doppler shifts in the signal. However, this effect is normally at a timescale much longer than those at which the curvature is being observed (days for Cassini, hours to minutes for LISA).

Much worse is the effect of non-gravitational forces that push the particles away from their geodesics. For slow particles, these induce a frequency variation with time of

$$\frac{1}{\omega_0}\frac{d\omega}{dt} \approx \frac{1}{c}\left[\left(\frac{\mathbf{F}}{m}\right)_{\mathrm{em}} - \left(\frac{\mathbf{F}}{m}\right)_{\mathrm{rec}}\right] \cdot \hat{n}_{\mathrm{ray}} \tag{4}$$

where $\mathbf{F}$ is the ordinary, non-gravitational force, m is the mass of the particle, em stands for the particle emitting the light ray, rec for the one receiving it and finally $\hat{n}_{\mathrm{ray}}$ is the unit vector in the ray's direction. Thus, stray forces, or accelerations, will mimic curvature signals.

This is not the only source of error when measuring curvature. Any instrumental frequency fluctuation directly spoils the measurement by mimicking a relative acceleration. This is the reason that normally null measurements are performed by comparing the change to a reference in an interferometer or taking the difference between two arms. Thereby, in order to measure curvature, two essential ingredients are required:

– free-falling test mass pairs with very low relative acceleration of non-gravitational origin,
– the ability of tracking these test masses with light-beams with very small instrumental fluctuations.

LISA Pathfinder aims at demonstrating both of these at an unprecedented level. In particular, LISA Pathfinder will demonstrate immunity from relative accelerations of non-gravitational origin to

$$\Delta a \leq 3 \times 10^{-14} \sqrt{1 + \left(\frac{f}{3\,\mathrm{mHz}}\right)^2}\ \mathrm{ms}^{-2}/\sqrt{\mathrm{Hz}} \tag{5}$$

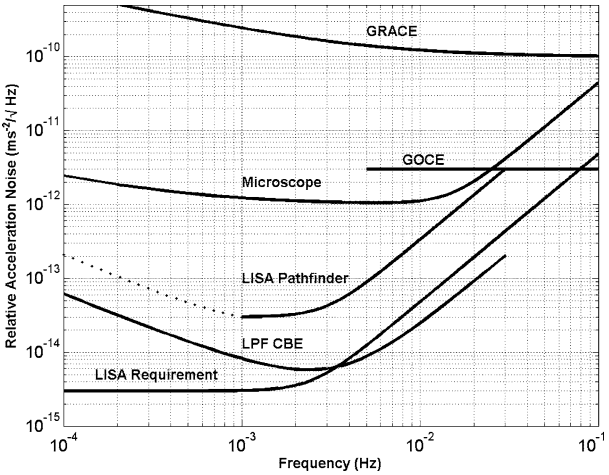

Fig. 5 Comparison of the performance of several missions. The line labelled *LPF CBE* is the current best estimate of the expected performance of LPF, the line labelled *LISA Pathfinder* is the LPF science requirement

over the frequency bandwidth of 1–30 mHz. *This is the top-level science requirement of the mission*. It should be noted that this requirement is a factor of ten less stringent than LISA, both in frequency and performance. However, as seen in Fig. 5, the current best estimate of the performance we can achieve from LISA Pathfinder is significantly better than the requirements. The final step to the required LISA performance will be performed via extrapolation.

In addition, LISA Pathfinder will demonstrate the ability of tracking free-floating test masses by laser interferometry with a resolution of

$$\Delta x \leq 9 \times 10^{-12} \sqrt{1 + \left(\frac{3\,\mathrm{mHz}}{f}\right)^2}\ \mathrm{m}/\sqrt{\mathrm{Hz}} \tag{6}$$

over a frequency bandwidth of 1–30 mHz with a dynamic range on the order of a millimetre.

Here, the main challenge is the low frequency at which this performance is required. Achieving low stray accelerations and low displacement noise becomes increasingly difficult at the lowest frequencies. Resolutions of better than $10^{-18}\,\mathrm{m}/\sqrt{\mathrm{Hz}}$ are routinely achieved by the LIGO, VIRGO and GEO 600 ground-based interferometers (Abramovici et al. 1992; Acernesse et al. 2004; Danzmann et al. 1992), but at frequencies above 100 Hz. However, all effects of interest for space missions are comparatively slow processes as they involve the motion of large bodies.

Several other missions have been flown, or are under development, which will use tracking of the relative motion of nearly free-falling artificial bodies. A comparison of the expected performance of these missions versus LISA Pathfinder is shown in Fig. 5. It is important to stress that LISA Pathfinder is not a mission mainly aimed at demonstrating drag free control. Drag-free control is just one of the many tools used to achieve test mass geodesic motion. *The main difference is that geodesic motion is the lack of relative acceleration between free test masses other than due to spacetime curvature, while drag free motion is the lack of acceleration of the spacecraft relative to a local inertial frame.*

LISA Pathfinder is both a mission in general relativity and in precision metrology, pushing these disciplines several orders of magnitude beyond their current state of the art. In doing so, it opens new ground for an entire class of new missions in general relativity, in fundamental physics at large, and in Earth observation (Drinkwater et al. 2003).

Also, it must be stated that the true objective of LISA Pathfinder is not to develop hardware, but to confirm the overall physical model of the forces that act on a test mass in interplanetary space. To fulfil this program, the mission is not going to just make a measurement of acceleration but will implement a full menu of measurements: at the end of this set of measurements, the residual acceleration noise model will be verified down to painstaking detail.

3 Mission Description

The main requirements for the LISA Pathfinder mission have been described in Sect. 2, but the most important of all is the level of free-fall purity as expressed by (5). This requirement dictates some fundamental constraints to the mission. Financial constraints prevented from baselining a similar orbit to LISA for LISA Pathfinder, as the launch energy and communication requirements would imply a large launcher and a complex and heavy platform. On the other hand, the requirements of LISA Pathfinder are not as demanding as those of LISA. A small launcher can easily bring a satellite into an earth orbit. The orbit should, however, be as far as possible free from eclipses, in order to maintain a stable thermal environment. In addition, the earth must be distant enough to avoid gravitational and magnetic disturbances. All these considerations and other more detailed ones, led us to choose a Lissajous orbit around the first Sun–Earth Lagrangian point (L1). This orbit, depicted in Fig. 6, maintains a stable environment; the distance from the Earth ranging between 1.2 to 1.8 million km does not require sophisticated communication equipment. The use of a small launch vehicle requires that the spacecraft is deployed into a relatively low Earth orbit, from where the spacecraft, with its own means, must travel to the operational orbit around L1. This transfer cost in terms of ΔV is about 3100 ms^{-1} and can be performed by means of several perigee burns (around 12) with a chemical bi-propellant engine providing 400 N thrust. The amount of propellant needed is rather large (see Table 1) and requires large tanks which at the end of the burn will still contain some fuel residual which might cause gravitational disturbance to the LTP experiment (see Sect. 4). The consequence is therefore that the propulsion module used for the transfer must be jettisoned from the science spacecraft where the LTP is accommodated before the science operational orbit is reached. The LISA Pathfinder spacecraft is therefore made of two modules as shown in Fig. 7. The propulsion module height is 2.4 m and the outer diameter is 2 m. The science spacecraft is described in more detail in Sect. 5.

The small launch vehicle selected is the new ESA small launcher VEGA. LISA Pathfinder is planned to be launched at the end of 2011, or early thereafter, from the European spaceport of Kourou (French Guyana) into a parking orbit with perigee at 200 km, apogee at 1620 km, and an inclination to the equator of 5.3°. Since the VEGA launcher is still under development, a back-up launch possibility is maintained with the Russian vehicle Rockot, which could launch LISA Pathfinder from Plesetsk (Russia) into a parking orbit with perigee at 200 km, apogee at 900 km, and an inclination to the equator of 63°. The apogee raising manoeuvres will last about 2 weeks and the transfer to L1 will take in total approximately 2 months from launch. Once in operational orbit, LISA Pathfinder will start the calibration phase and the experiment runs. This phase is planned to be completed in 6 months. The flight operations will be conducted by the European Space Operations Centre (ESOC) in Darmstadt (Germany), while the science operations are coordinated from the European Space Astronomy Centre (ESAC) in Villafranca (Spain).

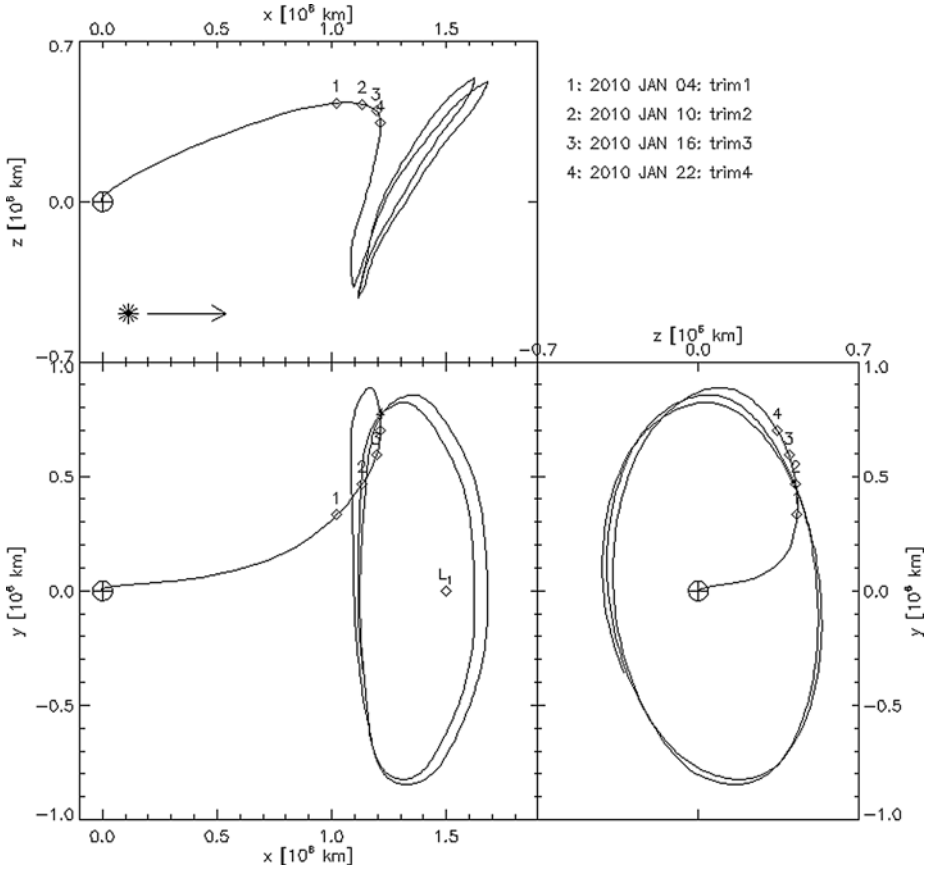

Fig. 6 Reference trajectory for LISA Pathfinder. The trajectory is shown in synodic (co-rotating) frame with the Earth at the origin, the x-axis pointing into the Sun direction, and the x–y plane being the plane of the ecliptic. The z-axis (out-of-plane axis) is chosen to form a right-handed coordinate system. The *markers* show the positions of the spacecraft at different epochs

4 LISA Technology Package

Unlike traditional observatory or planetary missions, the payload in LISA Pathfinder cannot be considered as a discrete piece of hardware carried by the spacecraft. Instead, during science operations, the payload and the spacecraft act as a single unit: the attitude control of the spacecraft is driven by the payload. LISA Pathfinder will carry two payloads; the LISA Technology Package (LTP), and the Disturbance Reduction System (DRS). Only the LTP will be described here.

The LISA Technology Package is provided by a consortium of European National Space Agencies and ESA. Table 2 lists the countries, institutes/industries, and responsibilities, involved in the manufacture of the LTP.

As described earlier in this paper, the main aim of LISA Pathfinder is to demonstrate the principle of geodesic motion to more than two orders of magnitude better than has been previously achieved. In order to meet this goal, all external forces acting on the test mass must be reduced to level below which the relationship in (5) can be met. LTP has been

Table 1 LISA Pathfinder mass budget

Item	Maximum mass [kg]
Data handling	15.4
Power subsystem	63.1
X-Band comms subsystem	8.3
AOCS	17.5
Structure	83.0
Thermal subsystem	8.8
Micropropulsion subsystem	43.8
Balance mass	17.5
LISA technology package	150
Disturbance reduction system	43
Science spacecraft dry total	450.4
Structure	81.4
Main engine	100.3
Thermal subsystem	10.6
Harness	8.5
Separation system	8.5
Propulsion module dry total	209.3
Propellant	1214.0
Launch composite wet total	1873.7
Launch vehicle capability	1910.0
Wet mass margin	36.3

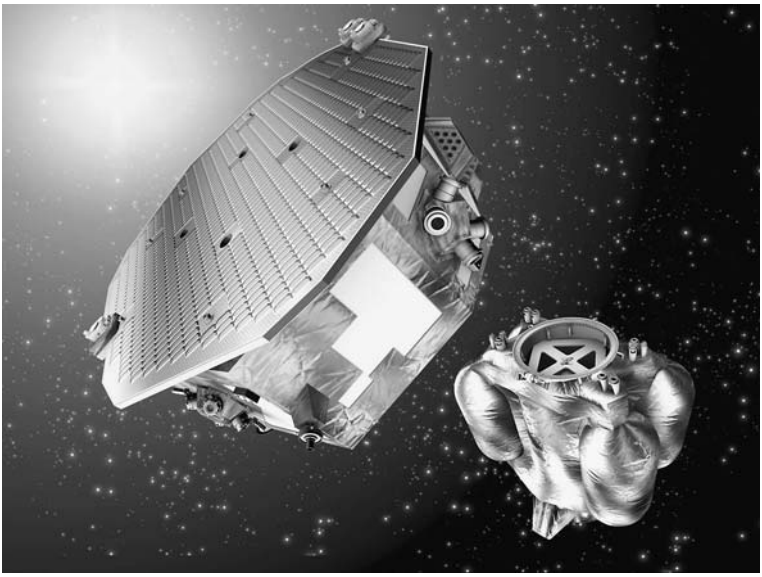

Fig. 7 Artist impression of the LISA Pathfinder after separation of the science module from the propulsion module, before reaching the operational orbit around L1

designed to meet these stringent requirements. The main role of the LTP is to house the test masses and provide the position information of the test masses to the Drag-Free and Attitude Control System (see Sect. 5.2). However, due to the resolution required, coupled with the

Table 2 Responsibilities in the manufacture of the LISA Technology Package

Country	Institute/Industry	Responsibility
France	APC, Paris, Oerlikon (CH)	Laser Modulator
Germany	AEI, Hanover	Co-PI, Interferometer design
	Astrium GmbH	LTP Architect
	Tesat	Reference Laser Unit
Italy	University of Trento	PI, Inertial Sensor Design
	Carlo Gavazzi Space	Inertial Sensor Subsystem (ISS)
	Thales Alenia Space	Test Mass
		Electrode Housing
The Netherlands	SRON	ISS Check Out Equipment
Spain	IEEC/University of Barcelona	Data Management Unit
		Data Diagnostic System
Switzerland	ETH Zurich/Oerlikon	ISS Front End Electronics
United Kingdom	University of Birmingham	Phasemeter Assembly
	University of Glasgow	Optical Bench Interferometer
	Imperial College London	Charge Management System
ESA	Thales Alenia Space	Caging Mechanism
	Astrium GmbH	LTP Architect

proximity of hardware to the test masses, the performance and environmental requirements levied on the LTP subsystems is extremely demanding.

Figure 8 shows an artists impression of the LTP. The LTP consists of two major subsystems; the inertial sensor subsystem, and the optical metrology subsystem. Both subsystems are described in further detail in the following sections.

4.1 Inertial Sensor Subsystem

The inertial sensor subsystem consists of the test masses and all systems interacting directly with the test masses, i.e. the electrode housing, front-end electronics, vacuum system, charge management, and caging mechanism. This section will describe each of these subsystems in turn.

In LISA Pathfinder, the test masses consist of a 1.96 kg cube of gold:platinum monophasic alloy of dimension 46 mm on a side. The alloy is formed from 73% gold and 27% platinum, chosen as this material can have an extremely low magnetic susceptibility ($\chi_m \approx 10^{-5}$) and high density $\approx 20\,\mathrm{kg\,m^{-3}}$. The combination of both greatly reduces the effect of external forces on the test mass. A detailed description of the noise sources affecting the test masses is beyond the scope of this paper. The reader is directed to Brandt et al. (2008) for the full error budget of the noise sources affecting the performance of the mission.

The position of the test masses is readout by two means: high resolution laser interferometry, and electrostatic (capacitive) sensing. The former only senses the test mass position

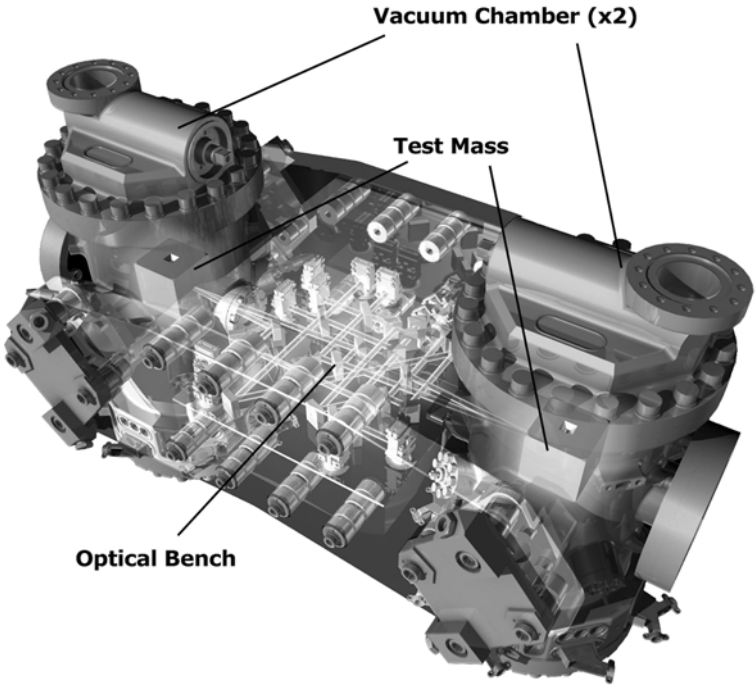

Fig. 8 Artists impression of the LISA Technology Package

along the sensitive axis (the line joining the two test masses) and the angles of rotation around the axes perpendicular to the sensitive axis, whereas the capacitive sensor measures the position of the test mass in all six degrees of freedom. The capacitive sensor comprises a hollow cubic molybdenum housing with gold coated sapphire electrodes mounted in the faces (see Fig. 9). The housing is sized to allow for a 4 mm gap between the electrode faces and the test mass. The size of the gap is a trade off between reducing the effects of noise sources, e.g. from uncontrolled potentials on the electrodes, and being able to meet the capacitive sensing requirement of $2\,\mathrm{nm}/\sqrt{\mathrm{Hz}}$ over the measurement bandwidth.

The capacitive readout system, known as the *Inertial Sensor Subsystem Front End Electronics* (ISS FEE), is arranged such that electrodes facing opposing faces of the test mass are combined via a capacitive bridge. A change in the position of the test mass gives a differential, bi-polar, signal. As well as sensing the position of the test masses, the ISS FEE can also be used to actuate (force) the test mass. In the basic operational mode of LISA Pathfinder, one test mass can be considered drag free, i.e. the position of this test mass with respect to the spacecraft is fed back to the thrusters such that the *spacecraft* is forced to follow the test mass. However, in this case, any unbalanced external force acting on the second test mass will cause a differential motion between the drag-free mass and the second test mass, which, if uncontrolled, will lead to a collision with the electrode housing after a period of time. For this reason, the ISS FEE must force the second test mass back to the optimum location within the electrode housing. However, this feedback loop only acts at frequencies below the measurement bandwidth, in order not to add noise at the frequencies of interest.

The test mass and electrode housing are mounted inside a dedicated vacuum enclosure. In order to meet the instrument requirements, the vacuum around the test mass must be maintained, throughout the mission lifetime, to less than 10^{-5} Pa. While inter-planetary space is

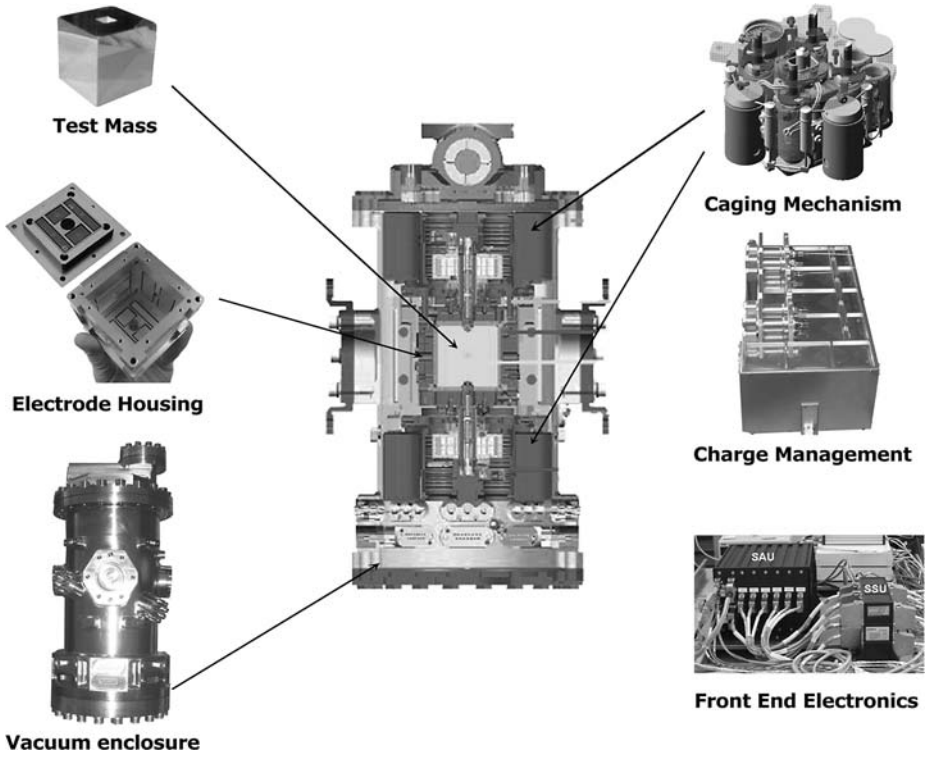

Fig. 9 The Inertial Sensor. The centre graphic shows a cut-away of the Inertial sensor vacuum enclosure. The photographs around the side show engineering models of the ISS subsystems (with the exception of the drawing of the caging mechanism which is shown for clarity)

an exceptionally good vacuum environment, the space inside, and around, a spacecraft is considerably more dirty (due to outgassing) than can be tolerated by the LISA Pathfinder inertial sensor, hence the need for a dedicated vacuum chamber. As with all equipment used in LISA Pathfinder, only non-magnetic materials can be used in the system, forcing the vacuum chamber to be manufactured from titanium as opposed to the standard stainless steel construction techniques. Also, in order to limit the pressure increase due to outgassing or virtual leaks within the vacuum enclosure (see Fig. 9), a getter pump assembly is required to keep the vacuum at the required level.

As there is no physical contact between the test mass and the surrounding environment, one issue that must be dealt with is charging of the test mass due to cosmic ray and solar energetic particle impacts. A build up of charge on the test mass, coupled with the potentials on the electrodes, will lead to additional noise in the test mass position. The actual charge on the test mass is measured by commanding the test mass to rotate with a given amplitude and looking at the corresponding actual displacement of the mass. The difference between the commanded and actual motion provides a measure of the test mass charge. The charge is then controlled using a non-contact discharge system based on the photo-electric effect. UV light from Mercury vapour lamps is channelled to the electrode housing via fibre optic cables. Depending on the sign of the charge on the test mass, the light is either shone onto the test mass or the electrode housing. The system has two modes of operation: rapid discharge, where the science run is stopped, the charge measured, and the UV lamps set to near

maximum intensity to discharge the mass in as quick a time as possible; and a continuous discharge mode, where the science measurement is not interrupted, the mass is forced to rotate around the x-axis (direction θ in Fig. 11) and the UV lamps are set to a low intensity such that the charging rate is balanced, preventing charge build-up on the mass. Both schemes will be tested on LISA Pathfinder.

A further challenge which is unique to space flight hardware is the need for a launch-lock device to prevent hardware being damaged during the extreme vibration conditions experienced at launch. In LISA Pathfinder, this is especially true for the test masses—the most sensitive part of the experiment must survive a random load of $\approx 50\,g_{rms}$, requiring a holding force of ≈ 2000 N, while not damaging the gold coated surface of the cube. In addition to the launch load requirement, when on-orbit, the device must release the test mass within an error box of 200 micron, with a velocity of less than $5 \times 10^{-6}\,ms^{-1}$. These requirements are met by the *Caging Mechanism Assembly*. This device consists of three actuators: a first stage hydraulic actuator to provide the 2000 N pre-load; a second stage positioning actuator, which is used to break the adhesion of the launch lock, and position the test mass to the desired location; and finally, the release actuator, a small diameter pin which is used to break the adhesion of the positioning plunger, and release the mass with the required accuracy. The caging mechanism is shown in Fig. 9.

Several other challenges must also be solved in order to meet the requirements of the LTP. These include: balancing of the differential gravitational force and gradient at the test mass positions—achieved by mounting compensation masses inside, and external to, the vacuum enclosure; creating a thermally quiet environment around the test mass—a temperature stability of $10^{-5}\,K/\sqrt{Hz}$ over the measurement bandwidth is required; associated with the thermal stability requirement is the need to have thermometers with a resolution better than $10^{-5}\,K/\sqrt{Hz}$; and as mentioned earlier, no magnetic materials can be used—this makes the design of several of the subsystem units especially difficult (e.g. vacuum chamber/pumps, mounting brackets, bolts, etc.).

4.2 Optical Metrology Subsystem

The Optical Metrology Subsystem (OMS) is the high resolution laser interferometric read-out of the test-mass positions. The OMS comprises several subsystems, namely; the reference laser unit, the laser modulator, optical bench interferometer, and the phase meter.

The *Reference Laser Unit* (RLU) employed on LISA Pathfinder is a 35 mW Nd:YAG non-planar ring oscillator (Kane and Byer 1985) of the same design commonly used in metrology labs around the world. This laser design is ideal for space applications due to its small size, high electrical to optical efficiency, and inherent low noise operation. The challenges for space applications come from the need for a robust design which can survive both the launch loads and thermal environment, as well as having a sufficient lifetime to guarantee the life of the mission. All of these challenges have been overcome and similar lasers are now flying in space on optical communication satellites (Heine et al. 2006).

The RLU output is fibre coupled using single-mode, polarisation-maintaining fibre. The fibre couples the light to the subsequent component in the optical chain, the *Laser Modulator* (LM). The LM consists of a beam splitter, two acousto-optic modulators, and optical pathlength actuators. The light from the laser is split into two paths, each path is passed through an acousto-optic modulator (also known as a frequency shifter). One modulator is driven at 80 MHz, while the other is driven at 80 MHz + 1.2 kHz, thereby creating two beams with a frequency difference of 1.2 kHz. The beams are then passed through the optical pathlength difference (OPD) actuator which consists of a fibre optic cable wrapped around a cylindrical piezo-electric transducer. The OPD is used to stabilise the fibre optic paths leading to

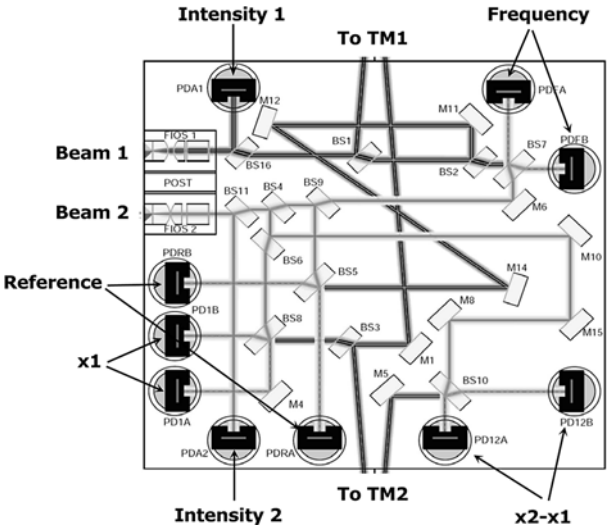

Fig. 10 Optical Bench Interferometer layout. The labels *To TM1* and *To TM2* indicate the positions of the test masses (not shown)

the optical bench. After the OPD, the beams are transmitted, again via sm/pm fibre, to the *Optical Bench Interferometer* (OBI).

The main function of the OBI is to direct the beams to the relevant positions in 3-dimensional space, without adding any significant noise to the measurement path. The primary optical bench requirement can be stated that the pathlength noise induced by the components on the optical bench should not exceed $1\,\mathrm{pm}/\sqrt{\mathrm{Hz}}$ [1] over the measurement bandwidth. The optical bench is constructed from a block of Zerodur ceramic glass measuring $200 \times 212 \times 22.5\,\mathrm{mm}$. Fused silica mirrors and beamsplitters are used to reflect the two beams to form four interferometers on the bench: the $x_2 - x_1$ interferometer which measures the differential motion of the two test masses—this is the primary science measurement of the mission; x_1 interferometer which measures the position and angles of test mass 1 with respect to the optical bench (and, therefore, the spacecraft); the *Frequency* interferometer which is an unequal arm Mach–Zehnder interferometer, sensitive to laser frequency fluctuations—the output of this interferometer is used to stabilise the laser frequency; and the *Reference* interferometer which is a rigid equal arm interferometer which provides the system noise floor, and is used to stabilise the fibre pathlengths via the OPD. The light from each fibre is also sent directly to a photodiode which is used to monitor the laser intensity noise. The signal from these photodiodes is used to stabilise the intensity of both beams by feeding back to the acousto-optic modulator drive signal. Figure 10 shows the optical layout of the optical bench with each of the interferometers labelled.

The signals from the (quadrant) photodiodes of each interferometer (each interferometer has two quadrant photodiodes for redundancy) are sent to the *PhaseMeter Assembly*. The phasemeter samples the data at 100 Hz and performs a single bin discrete Fourier transform to measure the phase of the signals at the heterodyne frequency. This technique is used due to the efficiency of the algorithm. The phasemeter not only outputs the longitudinal phase from the respective interferometers, but also outputs the angles between the wavefronts interfering on the photodetectors—commonly known as *differential wavefront sensing* (DWS). The latter signals from the x_1 and $x_2 - x_1$ interferometers are used to align the test mass to

[1] pm = pico-metre ($\equiv 10^{-12}$ m).

the interferometer. The longitudinal signals from the interferometers are used to stabilise the laser frequency, the optical pathlength, and (with the DWS signals) as inputs for the DFACS.

As mentioned above, the phasemeter samples the data at 100 Hz. However, the 100 Hz samples are not required for routine operation, and so the data is downsampled to 10 Hz prior to transmission to the on-board computer (and hence the DFACS). The downsampling is performed inside the *Data Management Unit* (DMU)—a 12 MHz ERC32 processor. The DMU is also responsible for the interface to the LTP subsystems, routing telecommands and timing information to the units, and collecting and transmitting telemetry to the on-board computer. The DMU also controls the diagnostic subsystems, consisting of heaters/ thermometers, coils/magnetometers, and a radiation monitor. The diagnostic items are required to isolate particular noise sources in the LTP.

5 Spacecraft

The science module carries all the necessary subsystems required to support the performance of the scientific experiments. In addition, this module is also supporting with power and command and data handling the operations of the propulsion module until separation. The science module moreover physically hosts the LTP and the American payload, the Disturbance Reduction System (DRS). The DRS replicates some of the functions of the Drag-Free Attitude Control System (DFACS), including using the LTP as the inertial sensor. The science module also hosts an American micro-propulsion system, the Colloidal Micro-Newton Thrusters (CMNT). In this paper, we are going to emphasise the technology associated with the spacecraft, therefore, in the following a general overview is given on the *standard* platform followed by a more detailed description of the micro-propulsion system and the drag-free attitude control system.

5.1 Spacecraft Platform

The Science Spacecraft platform structure provides the mechanical support for the hardware of the other spacecraft subsystems. The spacecraft has a shape of an octagonal prism. The outer diameter is 231 cm and the height 96 cm. One of the two bases is covered by a sunshield panel supporting an array of triple-junction GaAs solar cells of 2.8 m^2, providing at end-of-life 650 W of power, while the other base interfaces with the propulsion module. A large central cylinder accommodates the LTP Core Assembly, while the rest of the payload equipment and the spacecraft units are mounted as far away as possible on shear walls connecting the central cylinder to the outer panel forming the octagonal structure. The cylinder and all structural panels are constructed from sandwich panels or shells with carbon fibre laminate skins bonded to aluminium honeycomb core. Aluminium items are limited to structural rings, cleats, inserts, and minor brackets.

The thermal control subsystem must guarantee the very stable thermal environment required by the science measurements. Together with the stringent thermal stability required at LTP level, as seen in Sect. 4.1, a stable thermal environment of $10^{-4}\,\mathrm{K}/\sqrt{\mathrm{Hz}}$ is also required at the LTP interface, in order to minimise the thermo-elastic distortions. Passive means are used to control the upper temperatures of sensitive equipment, with electrical heaters to control the lower temperatures. The entire module is wrapped in Multi-Layer Insulation (MLI) except for designated radiator areas designed to reject to space the excessive heat. The minimum necessary heater power is applied in the cold cases so that the lower

temperature of each unit is maintained toward the bottom of their allowable range. By using the full design temperature range of each unit in this way, the heater power requirement is minimised. Heater switching is not permitted during the payload science operations as the transient variations in temperature that happen as heaters switch can interfere with the payload measurements. On the sensitive equipment, different combinations of trimming heaters are used to obtained the required temperatures. On the micropropulsion systems (both FEEP and CMNT), a high frequency pulse width modulation control of the heaters is used. Heat pipes are avoided as they too would interfere with the measurements due to gravitational disturbance caused by the transfer of mass through the pipes.

The science module is a three-axis controlled spacecraft. Apart from the DFACS, which is described in Sect. 5.2, an Attitude and Orbit Control Subsystem (AOCS) is needed in order to control the launch composite (when the propulsion module is attached to the science module) and for the on-station phases when the drag-free conditions cannot be maintained. The AOCS uses as sensors two Autonomous Star Trackers, two Digital Sun Sensors (DSS) for sun acquisition and in safe mode and two Fibre-Optic Gyroscopes Units, required for certain phases where the optical sensors are inoperable due to high rates or eclipse. They are also needed to provide high bandwidth data during the main engine burn. The AOCS actuators are 4 pairs of 10 N bi-propellant thrusters located on the propulsion module and three clusters of 4 FEEP thrusters each located on the sides of the science module.

The power subsystem provides a stable regulated bus, with voltage regulation at 28 V DC. During the technology demonstration phase the spacecraft will be sun pointing, therefore all electrical power can be generated by the solar array. Battery power is only required during launch and early operations (LEOP), for eclipse periods during the transfer, during slews to and from engine firing attitude, while firing the engine, and for any anomalies during the on-station phase. For a nominal mission, the battery is only required during the initial phases of the mission, therefore, because of its low mass, and simple management, a Li-ion battery providing 400 W h is used.

The On-Board Computer (OBC) is the central control unit for all on board data handling activities, the attitude and orbit control subsystem (AOCS), the DFACS, and the management of the platform and payload equipment. Data handling functions mainly constitute of command distribution, telemetry acquisition and timing facilities during all phases of the mission. Furthermore, the OBC performs monitoring functions and depending the detection of failures provides safe system reconfiguration capabilities. The OBC consists of several independent redundant modules: two processor modules, each based on a single chip ERC32 central processing unit working at 22.5 MHz with 6 MB RAM, 1.5 MB EEPROM and 64 KB PROM; two telecommand, telemetry, and reconfiguration units containing 400 KB safeguard memory; four actuator and sensors interface modules and two mass memory units of 12.5 Gb.

The OBC interfaces with the spacecraft units and the LTP through a MIL-bus 1553B, while the internal backplane link uses the space-wire standard. The OBC hosts the On-Board Software (OBSW) which performs all the spacecraft and most of the LTP functions. Only the interferometric optical measurement and the diagnostic functions are performed inside the LTP Data Management Unit (DMU) as described in Sect. 4.2.

The communications subsystem works at X-band frequency (7230 MHz uplink and 8495 MHz downlink) and provides for commanding and housekeeping telemetry during LEOP, transfer, and on-station and also transmits science data telemetry whilst on-station. For LEOP, some phases of transfer and during on-station anomalies, omni directional coverage is required. Two hemispherical antennas are used for the omni-directional coverage allowing a maximum data rate of 60 ksymbols/s during LEOP and 1 ksymbols/s at L1.

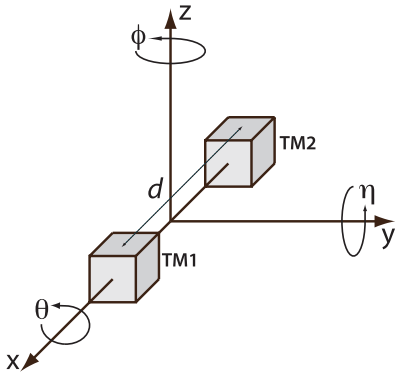

Fig. 11 LTP Test Masses layout schematic and axis rotation angles notation

However, to achieve the required telemetry data rate on-station at L1 distance, a medium gain horn antenna is used capable to transmit 120 ksymbols/s. Two X-band transponders are present for redundancy, with coherent ranging. Additional amplification is required at the output of the transponders to achieve the required telemetry margins.

5.2 Drag-Free Attitude Control System

The drag-free attitude control system is probably the single most important subsystem on board. The main objective of the DFACS is to control the spacecraft dynamics in such a way that the main requirement on the residual acceleration, expressed by (5) is met. Like any control system, DFACS makes use of sensors and actuators. The spacecraft attitude is sensed by means of a pair of star trackers with a measurement error of 32 arcsec/$\sqrt{\text{Hz}}$. With reference to Fig. 11, the test masses position (x_i, y_i, z_i with $i = 1, 2$) and attitude (θ_i, η_i, ϕ_i with $i = 1, 2$) with respect to their housing inside the inertial sensor, are sensed through two different means:

- *electrostatic readout* based on capacitance electronic measurement (see Sect. 4, with a measurement noise of 1.8 nm/$\sqrt{\text{Hz}}$ for x, y, z and 200 nrad/$\sqrt{\text{Hz}}$ for θ, η, ϕ
- *optical readout* based on laser interferometric measurement, with a noise of 9 pm/$\sqrt{\text{Hz}}$ for x_1 and $x_1 - x_2$ and 20 nrad/$\sqrt{\text{Hz}}$ for $\eta_1, \phi_1, \eta_{1-2}, \phi_{1-2}$

The actuation on the spacecraft attitude is performed by the set of micro-propulsion thrusters, described in Sect. 5.3, with a noise of 0.1 μN/$\sqrt{\text{Hz}}$. The forces and torques on the test masses are provided by the inertial sensor *electrostatic actuation*. During the science modes, the maximum differential acceleration noise allowed on the TMs is 10^{-14} ms$^{-2}/\sqrt{\text{Hz}}$.

The DFACS tasks is to control the 15 degrees of freedom (DOF) present on-board (6 DOF per test mass and 3 DOF for the attitude of the spacecraft) to fulfil the following objectives:

- to shield one test mass—the *drag-free* or *free floating* test mass—from external disturbances in the measurement bandwidth [1 mHz to 30 mHz]. The spacecraft is therefore controlled to follow the drag-free test mass, which is free to float in its housing, only subject to the forces that directly impact on the test mass (e.g. thermal radiation pressure, magnetic field interaction with TM), called internal forces f_i and to the non-contact coupling with the electrodes housing (e.g. due to electrostatic field and gravity gradient), called parasitic stiffness ω_i^2.

– to measure by laser interferometer the differential acceleration between the drag-free test mass and the second test mass maintained centred in its housing using electrostatic capacitive forces.
– to keep the spacecraft pointed to the Sun and the fixed communication antenna pointed to Earth.

This is realised by careful selection of the drag-free degrees of freedom and frequency band separation. The drag-free DOF conditions are not belonging to one TM, but on 6 DOFs of the two TMs: $x_1, y_1, z_1, \theta_1, y_2, z_2$. Below the measurement bandwidth the test masses drag-free DOFs $\theta_1, z_1 - z_2, y_1 - y_2$ are controlled using capacitive suspension control in order to maintain the attitude of the spacecraft according to the star tracker measurements and attitude guidance law. Above the measurement bandwidth, the spacecraft is controlled by means of the micro-propulsion system.

The drag-free controller design is not described in this paper but can be found in the literature (e.g. Fichter et al. 2005, 2007a, 2007b). The DFACS has several modes of operation, which are not described here in detail, and are used during the on station operations after release of the TM from the caging mechanism. One particular science mode, dubbed M3, is particularly interesting for the characterisation of the spurious acceleration noise acting on the TMs. In the M3 mode, the distance between the two TMs, measured by the interferometer, is used by the controller as the main signal to control the position of the spacecraft and of the suspended test mass. Neglecting the thermo-elastic deformation of the inertial sensors and optical bench and the cross-talk terms, the interferometer readout measurement equation is the following:

$$S = \frac{1}{s^2 + \omega_2^2 + \omega_{lfs}^2}\left[\frac{f_2 - f_1}{m_{TM}} + x_{nl}(s^2 + \omega_2^2) + \frac{\omega_2^2 - \omega_1^2}{s^2 + \omega_1^2 + \omega_{fb}^2}\left(\frac{F_{SC}}{M} + \omega_{fb}^2 x_n - \frac{f_1}{m_{TM}}\right)\right] \tag{7}$$

$S = x_1 - x_2 + x_{nl}$	is the interferometer differential measurement signal
x_i	is the displacement of the test mass i with respect to the inertial frame
$s = j\omega = 2j\pi f$	is the complex frequency
ω_i^2	is the parasitic stiffness of the test mass i
f_i	are the disturbance forces acting directly on the test mass i
F_{SC}	are the disturbance forces acting directly on the spacecraft
ω_{fb}^2	is the open loop drag free gain
ω_{lfs}^2	is the open loop electrostatics suspension gain
x_{nl}	is the noise of the differential laser interferometer
x_n	is the readout noise of the sensor used for the drag free (either electrostatic or interferometer)
m_{TM}	is the mass of the test mass
M	is the mass of the spacecraft

From (7), we can observe that there are three main contributions to the measured signal, which should be as low as possible, as it is directly related to the residual differential acceleration. The first is a combination of the direct internal forces acting on the test masses, the second is a term proportional to the differential interferometer noise and the third is the so-called spacecraft jitter noise, the physical movement of the TM along the measurement axis. It is instructive to examine these terms one by one. The first term, the internal forces contribution, enters into the equation without multiplying factor, so it cannot be minimised,

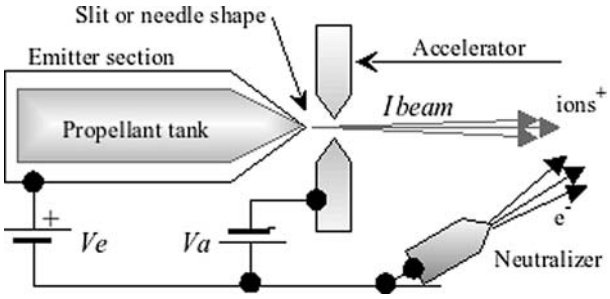

Fig. 12 FEEP propulsion concept

with respect to other contributors, by tuning system parameters. This means that the term has to be minimised by design and by proper selection of TM material and inertial sensor construction. The multiplying term of (7) can indeed reduce the effect of all the contributions, however, at a given frequency band, one can only tune the gain of the electrostatic suspension ω_{lfs}^2, which cannot be increased indefinitely. In other words, if the internal forces term is too large by LTP and system construction, it cannot be mitigated by system tuning. The second term is due to the interferometer noise. This is more important at high frequencies and at large ω_2^2. However, the intrinsic noise of the interferometer given by (6) makes this term rather small. The third contribution is dominated by the disturbance forces on the spacecraft (e.g. solar pressure fluctuations and micro-propulsion force noise) and by the noise of the measurement system used for the drag free control. In the case where the interferometer is used, the term x_n is small and the only remaining term is F_{SC}. This term can be minimised by tuning two system parameters: the difference between the parasitic stiffness $\omega_2^2 - \omega_1^2$ and the drag free gain ω_{fb}^2. The first term must be minimised, while the second maximised.

The above illustrates the basis upon which the on-board calibration and scientific runs will be performed and how the system will be tuned for optimal performance.

5.3 Micropropulsion

The LISA Pathfinder Micro-Propulsion Subsystem (MPS) is based on Field Emission Electric Propulsion (FEEP) technology. An extensive account can be found in Nicolini (2007) and Ceruti and Nicolini (2008). In field emission electrical propulsion, positive ions are directly extracted from liquid metals (Caesium for slit FEEP and Indium for Needle FEEP) and accelerated by means of electrostatic force in high vacuum. This function is carried out applying a very high voltage to a suitable electrode configuration, which is able to create and enhance very high electrical fields (up to 10^9 V/m). The FEEP working principle is given in Fig. 12. An additional external source of electrons, the neutraliser, needs to be included to maintain balanced the overall electrical charge of the system ($\text{ions}^+ = \text{e}^-$).

The main performance requirements of the propulsion system are shown in Table 3.

In addition to the performance requirements, the MPS once initialised and operating in orbit, must not have moving parts, nor gas leaks that could result in spacecraft disturbance and to avoid magnetic disturbance the thruster does not make use of ferro-magnetic materials.

The LISA Pathfinder MPS is composed of three main parts, called Micro Propulsion Assembly (MPA): each one consisting of one FEEP Cluster Assembly, one Power Control Unit (PCU) and one Neutraliser Assembly (NA). The FEEP Cluster Assembly (Fig. 13) consists of a self-contained unit of 4 FEEP Thrusters Assembly, which include propellant reservoir, mounted on a support structure. The four thrusters are devoted to provide thrust to the required vector directions and are commanded individually and work in hot redundancy.

Table 3 FEEP propulsion main requirements

Propulsion parameter	Requirement
Thrust range	0.1 μN to 150 μN
Thrust resolution	≤0.1 μN
Thrust accuracy	≤2% at max thrust
Thrust linearity	≤0.5%
Thrust response time	≤500 ms
Noise (from 10^{-4} Hz to 1 Hz)	$\leq 0.1\ \mu N/\sqrt{Hz}$

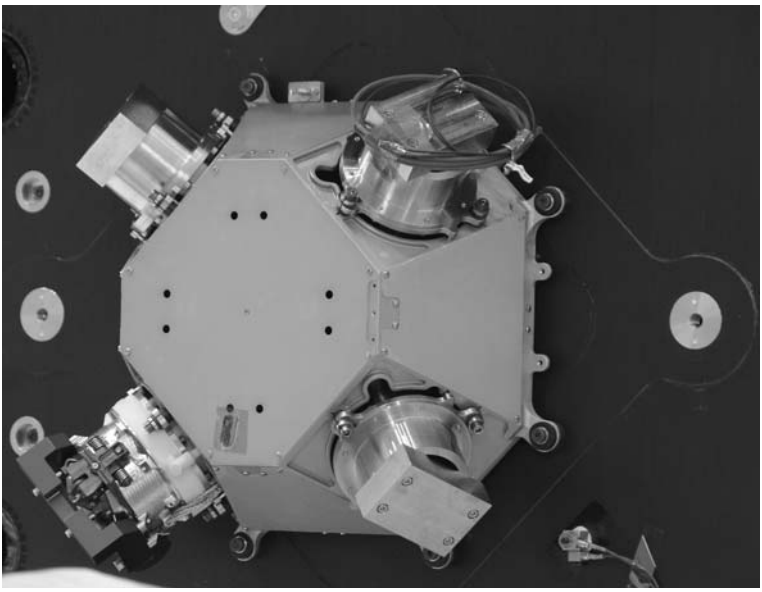

Fig. 13 Engineering Model of the Slit FEEP Cluster Assembly mounted on the spacecraft during the acoustic test at system level. The four thruster have the lids closed, as in launch configuration. A lid opening mechanism is operated before the thrusters can be used in orbit

The neutraliser assembly consists of a self-contained unit of two neutraliser units necessary to null the spacecraft imbalance due to ion thruster operations. Also, the neutralisation function is implemented by means of cold redundant hardware.

The power control unit consists of an electronic unit interfacing the spacecraft for power supply and telecommand and telemetry tasks and provide power and control to both FEEP Cluster and Neutraliser assemblies.

Each MPA is mounted at 120° with respect to the others. The PCU is located inside the spacecraft while the FCA and NA are mounted externally.

In order to characterise the thruster performance on ground, a complex instrument called the *Nanobalance* (NB) has been devised. The NB is based on a thrust stand with a dual pendulum balance where the plate deflection is measured by a Fabry–Perot interferometer. Designed to be able to measure accurately the full thrust range required down to a resolution fractions of micro-Newton, the NB has recently been upgraded to be able to measure the

thrust noise required (see Table 3). The system is based on multi-stage passive and active noise filtering array. A thrust stand, a vacuum system, a laser metrology system and a digital control unit basically compose the NB. More details and NB performance can be found in Canuto and Rolino (2004).

Acknowledgements The authors wish to acknowledge the instrumental role that the principal investigators of the LISA Pathfinder mission, Stefano Vitale of the University of Trento (I) and Karsten Danzmann of the Albert Einstein Institute of Hanover (D) play in this mission, together with the other members of the Science Working Team (Philippe Jetzer (CH), Alberto Lobo (E), Eric Plagnol (F), Martijn Smit (NL), and Harry Ward (UK)). The mission described in this paper is the result of the work of many ESA colleagues of the Science and Robotic Exploration Directorate at ESTEC, Noordwijk (NL) (Eliseo Balaguer, Denis Fertin, Cesar Garcia, Luisella Giulicchi, Rainer Gruenagel, Javier Huete, Bengt Johlander, Sean Madden, Davide Nicolini, Toni Romera, Hans Rozemeijer, Andreas Schoenenberg, Luca Stagnaro) and at ESAC, Villafranca (E) (Michele Armano, Jorge Fauste, Damien Texier), of the Technical Directorate at ESTEC (Mauro Caleno, Adrian Graham, Alfred Newerla, Zoran Sodnik, Laurent Trougnou, Shufan Wu, and many others) of the Operations Directorate at ESOC, Darmstadt (D) (Ian Harrison, Wolfgang Hell, Markus Landgraf, Mathias Lauer, Rolf Maarschalkerweerd, Andreas Rudolph, and many others). Furthermore, we gratefully acknowledge the work performed by the industrial consortium under the spacecraft platform prime-contractorship of Astrium Ltd. of Stevenage (UK) and LTP architect Astrium GmbH of Friedrichshafen (D).

References

A. Abramovici et al., LIGO: The Laser Interferometer Gravitational-Wave Observatory. Science **256**, 325 (1992)

F. Acernese et al., Status of VIRGO. Class. Quantum Gravity **21**, S385–S394 (2004)

B. Bertotti et al., A test of general relativity using radio links with the Cassini spacecraft. Nature **425**, 374–376 (2003)

N. Brandt et al., Experiment Performance Budget. LISA Pathfinder document S2-ASD-RP-3036 (2008)

S. Buchman et al., The Gravity Probe B Relativity mission. Adv. Space Res. **25**(6), 1177 (2000)

E. Canuto, A. Rolino, Nanobalance: An automated interferometric balance for micro-thrust measurement. ISA Trans. **43**, 169–187 (2004)

L. Ceruti, D. Nicolini, Power Processing Control Units for FEEP Micro-Propulsion Subsystems, International Astronautic Congress (Glasgow, October 2008)

K. Danzmann et al., The GEO Project: A long baseline laser interferometer for the detection of gravitational waves. Lect. Not. Phys. **410**, 184–209 (1992)

M. Drinkwater et al., GOCE: ESA's first Earth explorer core mission. Space Sci. Ser. ISSI **18**, 419 (2003)

A. Einstein, Preuss. Akad. Wiss. Berlin, Sitzungsberichte der Physikalisch-mathematischen Klasse, p. 688 (1916)

W. Fichter, P. Gath, S. Vitale, D. Bortoluzzi, LISA Pathfinder drag-free control system implications. Class. Quantum Gravity **22**(10), s139–s148 (2005)

W. Fichter, A. Schleicher, S. Vitale, Drag-free control design with cubic test masses, in *Lasers, Clocks, and Drag-Free Control*, ed. by H.J. Dittus, C. Lämmerzahl, S. Turyshev. Astrophysics and Space Science Library, vol. 349 (Springer, Berlin, 2007a). ISBN:978-3-540-34376-9

W. Fichter, A. Schleicher, S. Bennani, S. Wu, Closed loop performance and limitations of the LISA Pathfinder drag-free control system. AIAA 2007-6732, AIAA Guidance Navigation and Control Conference, 20–23 August 2007b, Hilton Head, South Carolina

F. Heine et al., Space qualified laser sources. Optical Sensing II. Proc. SPIE **6189**, 61892I (2006)

R. Hulse, J. Taylor, Astrophys. J. **195**, L51–L53 (1975)

T. Kane, R. Byer, Monolithic, unidirectional single-mode Nd:YAG ring laser. Opt. Lett. **10**(2), 65–67 (1985)

J. Mester et al., The STEP mission: principles and baseline design. Class. Quantum Gravity **18**, 2475 (2001)

W.-T. Ni, ASTROD—an overview. Int. J. Mod. Phys. D **11**, 947 (2002)

D. Nicolini, LISA Pathfinder field emission thruster system development program, in *30th International Electric Propulsion Conference*, IEPC-2007-363, Florence, 2007

A. Nobili et al., 'Galileo Galilei' flight experiment on the equivalence principle with field emission electric propulsion. Class. Quantum Gravity **13**, A197 (1996)

R.D. Resenberg et al., Viking relativity experiment: verification of signal retardation by solar gravity. Astrophys. J. **234**, L219 (1979)

D. Shaddock, Space based gravitational wave detection with LISA. Class. Quantum Gravity **25**(11), 114012 (2008)
R. Takahashi et al., Status of TAMA300. Class. Quantum Gravity **21**, S403–S408 (2004)
P. Touboul et al., MICROSCOPE, testing the equivalence principle in space. C. R. Phys. **2**, 1271–1286 (2001)
S.G. Turyschev et al., The laser astrometric test of relativity mission. Nucl. Phys. B **134**, 171 (2004)
S. Vitale et al., LISA Pathfinder: Einstein's Geodesic Explorer, ESA-SCI (2007), p. 1